Quaternary Science Reviews 59 (2013) 87–100

Contents lists available at SciVerse ScienceDirect

Quaternary Science Reviews

journal homepage: www.elsevier.com/locate/quascirev

Holocene temperature history at the western Greenland Ice Sheet margin reconstructed from lake sediments

Yarrow Axford [a,*], Shanna Losee [b], Jason P. Briner [b], Donna R. Francis [c], Peter G. Langdon [d], Ian R. Walker [e]

[a] Department of Earth and Planetary Sciences, Northwestern University, Evanston, IL 60208, USA
[b] Department of Geology, University at Buffalo, 411 Cooke Hall, Buffalo, NY 14260, USA
[c] Department of Geosciences, University of Massachusetts, Morrill Science Center, 611 North Pleasant Street, Amherst, MA 01003, USA
[d] Geography and Environment, University of Southampton, Highfield, Southampton SO17 1BJ, UK
[e] Palaeoecology Laboratory, University of British Columbia, Okanagan Campus, Kelowna, BC V1V1V7, Canada

ARTICLE INFO

Article history:
Received 27 February 2012
Received in revised form
15 October 2012
Accepted 19 October 2012
Available online 29 November 2012

Keywords:
Greenland
Jakobshavn
Holocene thermal maximum
Neoglaciation
Paleoclimate
Lake sediments
Chironomidae

ABSTRACT

Predicting the response of the Greenland Ice Sheet to future climate change presents a major challenge to climate science. Paleoclimate data from Greenland can provide empirical constraints on past cryospheric responses to climate change, complementing insights from contemporary observations and from modeling. Here we examine sedimentary records from five lakes near Jakobshavn Isbræ in central West Greenland to investigate the timing and magnitude of major Holocene climate changes, for comparison with glacial geologic reconstructions from the region. A primary objective of this study is to constrain the timing and magnitude of maximum warmth during the early to middle Holocene positive anomaly in summer insolation. Temperature reconstructions from subfossil insect (chironomid) assemblages suggest that summer temperatures were warmer than present by at least 7.1 ka (the beginning of the North Lake record; ka = thousands of years before present), and that the warmest millennia of the Holocene occurred in the study area between 6 and 4 ka. Previous studies in the Jakobshavn region have found that the local Greenland Ice Sheet margin was most retracted behind its present position between 6 and 5 ka, and here we use chironomids to estimate that local summer temperatures were 2–3 °C warmer than present during that time of minimum ice sheet extent. As summer insolation declined through the late Holocene, summer temperatures cooled and the local ice sheet margin expanded. Gradual, insolation-driven millennial-scale temperature trends in the study area were punctuated by several abrupt climate changes, including a major transient event recorded in all five lakes between 4.3 and 3.2 ka, which overlaps in timing with abrupt climate changes previously documented around the North Atlantic region and farther afield at ∼4.2 ka.

1. Introduction

Greenland's present-day climate and cryosphere are currently subjects of intensive investigation, in part because ongoing changes in the mass balance of the Greenland Ice Sheet have worldwide ramifications via contributions to global sea level (Alley et al., 2008; Rignot et al., 2011). Paleotemperature data, in combination with glacial geologic reconstructions, can help clarify how the Greenland Ice Sheet responds to climate change. Paleo-data provide empirical constraints on past ice-sheet responses to climate change (Long, 2009), and are useful for testing and improving general circulation models and the physics-based ice sheet models that are central to forecasting future mass balance changes (Simpson et al., 2009; Robinson et al., 2011).

The pre-industrial Holocene was characterized by changes in insolation and other climate forcings that caused significant climate changes in the Arctic and elsewhere (Kaufman et al., 2004; Mayewski et al., 2004; Renssen et al., 2009; Zhang et al., 2010). Thanks to widely preserved geologic archives, this most recent epoch of Earth's history provides opportunities to reconstruct those natural climate variations – and their impacts on ecosystems and ice sheets – in more detail than for earlier periods. Knowledge of Greenland's Holocene climate history comes from a combination of geomorphic and paleoecological evidence e.g., glacial deposits, beach ridges and remains of thermophilous species found north of their present-day habitat e.g. (Hjort and Funder, 1974; Bennike, 2004; Kelly and Lowell, 2009; Funder et al., 2011), ice sheet borehole temperatures (Dahl-Jensen et al., 1998), and continuous proxy

* Corresponding author. Tel.: +1 847 467 2268; fax: +1 847 491 8060.
E-mail addresses: axford@northwestern.edu, axford@colorado.edu (Y. Axford).

0277-3791/$ – see front matter © 2012 Published by Elsevier Ltd.
http://dx.doi.org/10.1016/j.quascirev.2012.10.024

records from ice cores, lake sediments, and marine sediments (e.g., Johnsen et al., 2001; Jennings et al., 2002; Andersen, 2004; Masson-Delmotte et al., 2005; de Vernal and Hillaire-Marcel, 2006; Moros et al., 2006; Wagner et al., 2007). Many records indicate that Greenland – like much of the Arctic and subarctic – experienced warmer summers for some portion of the early to middle Holocene, in response to high boreal summer insolation, and that early to mid-Holocene warmth was followed by cooling and glacier expansion in the late Holocene as summer insolation declined (Kaufman et al., 2004, 2009). The timing and magnitude of these changes were spatially variable (Kaufman et al., 2004; Kaplan and Wolfe, 2006; Renssen et al., 2009; Sundqvist et al., 2010), and remain uncertain in many parts of the Arctic.

Lake sediments from Greenland's ice-free margin provide continuous archives of past environmental change, including climate and glacier extent, which begin in the Lateglacial to middle Holocene depending on the timing of local basin deglaciation (Björck et al., 2002; Kaplan, 2002; Anderson et al., 2004). Here we present Holocene climate reconstructions from five lakes along the western Greenland Ice Sheet margin, near Jakobshavn Isbræ and Disko Bugt (Fig. 1). Insect (chironomid) remains from North Lake are used to generate quantitative estimates of summer temperatures. Changes in sediment composition at the five study lakes are interpreted as evidence for ice sheet fluctuations, changes in lake productivity, and regional climate changes throughout the Holocene.

2. Study sites

The landscape between Disko Bugt and the Greenland Ice Sheet margin comprises a ~25–40 km wide swath of ice-scoured exposed bedrock with sparse moraines, and is dotted with hundreds of lakes. This landscape is bisected by Jakobshavn Isfjord and Jakobshavn Isbræ, a major outlet glacier of the Greenland Ice Sheet (Fig. 1). The land surface throughout most of the region was deglaciated in the early Holocene following the last glaciation, when this sector of the Greenland Ice Sheet terminated on the continental shelf (Weidick and Bennike, 2007). Young et al. (2011a, 2011b) provide the most recent chronological control on deglaciation of the region: According to those results, following deglaciation of the coastal terrain fringing Disko Bugt ~10.2 ka (ka = thousands of years before present, calibrated age), the ice margin re-advanced to deposit the prominent Fjord Stade moraines at ~9.2 (Marrait moraine) and 8.2 ka (Tasiussaq moraine). These early Holocene advances were followed by ice retreat to a location inland of the present ice margin by ~7 ka. Accordingly, the timing of lake inception for the five study sites ranges from ~10 ka near the Disko Bugt coast (Pluto and Fishtote lakes) to ~7 ka near the present-day ice sheet margin (North, Iceboom and Loon lakes; Fig. 1). All five lakes in the present study lie well above the marine limit, at elevations between 170 and 285 m asl.

All lakes have surface areas <1 km^2, and lake depths range from 4.2 to 41 m (Table 1; all lake names are informal). Secchi depth measured at Fishtote Lake in August 2009 was 5.8 m; no other limnological data are available from the sites. The landscape surrounding each of the study lakes is dominated by scoured siliceous bedrock with very little soil cover and sparse low arctic tundra vegetation including heath and low willow scrub (Fig. 3). As can be seen in Fig. 3, there is subtle variation between sites, for example with sparser vegetation cover occurring at higher-elevation Fishtote Lake in comparison with North Lake. At the town of Ilulissat (Fig. 1), which is situated closer to the coast and at lower elevation than the study sites, mean July temperature for the years 1971–2000 was 7.7 °C and mean annual temperature was −4.8 °C.

The five study lakes were selected to represent a range of Holocene paleoenvironmental histories with respect to ice sheet influence: Fishtote and North lakes (Figs. 1–3) have not received

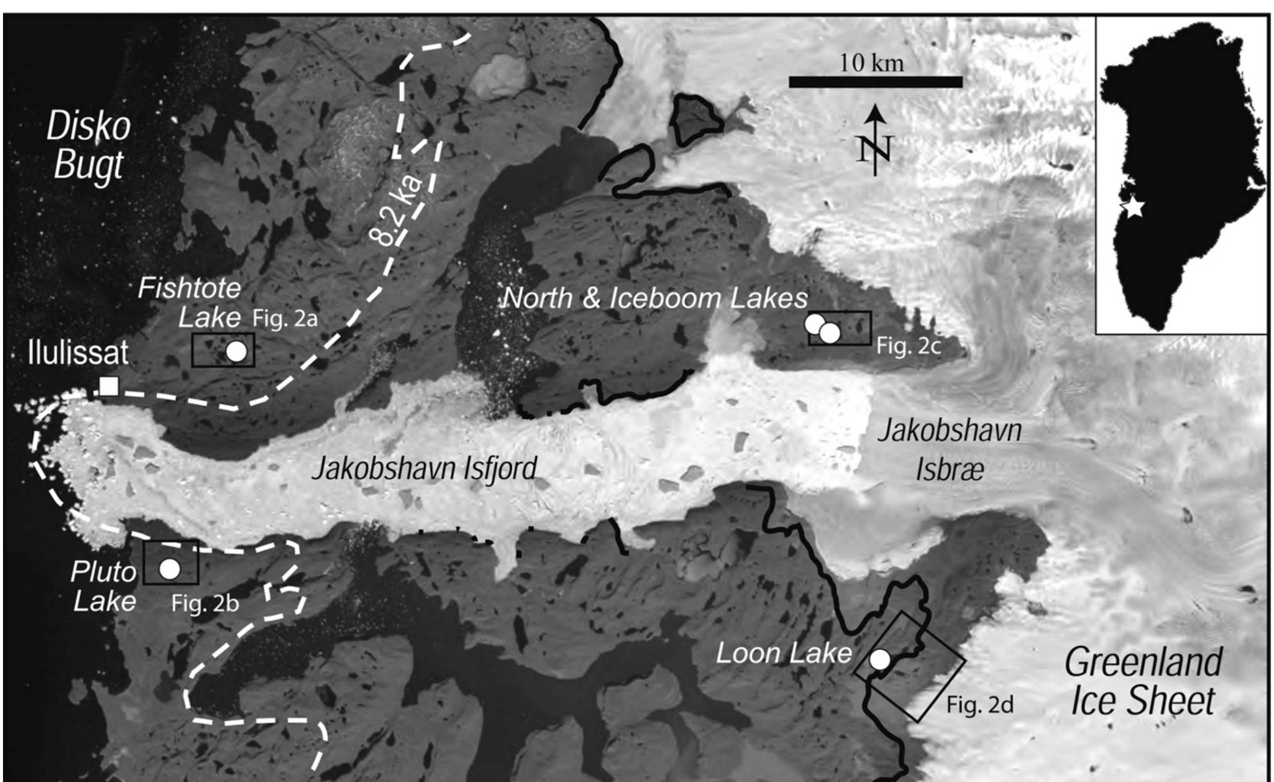

Fig. 1. Locations of the five studied lakes in the Jakobshavn region of West Greenland. Base image is 2001 LANDSAT. Dashed line shows the location of the ~8.2 ka Tasiussaq moraine; thick black line represents historical moraine.

Table 1
Lake site and sediment core descriptions.

Lake name	Elevation (m)	Latitude	Longitude	Lake surface area (km^2)	Lake maximum depth (m)	Water depth (m) at core site	Sediment core name(s)	Core length (cm)	Estimated basal age[a]
Loon Lake	278	69° 03.489′	−49°54.963′	0.42	Unknown	15.8[b]	08-LOO-1	77	6500 cal yr BP
Iceboom Lake	185	69°14.121′	−50° 00.953′	0.96	41.0	3.1[b]	08-ICE-5	76	7300 cal yr BP
North Lake	190	69°14.497′	−50° 01.634′	0.01	4.5	3.9	08-NOR-3	106	7340 cal yr BP
		69° 14.527′	−50° 01.823′			4.0	09-NOR-1	42	Surface core
Pluto Lake	170	69° 06.520′	−51° 01.829′	0.08	4.2	3.5	09-PLO-1	84	9210 cal yr BP
		69° 06.523′	−51° 01.820′			3.9	09-PLO-SC1	22	Surface core
Fishtote Lake	285	69° 13.688′	−50° 55.601′	0.07	10.9	9.2	09-FTL-SC2	118	9730 cal yr BP

[a] Basal ages are extrapolated from bottom-most ^{14}C ages. All five ^{14}C-dated cores have inorganic lacustrine sediments at their base.
[b] Core site within a sub-basin of the lake.

glacial meltwater since their initial Holocene deglaciation, so they preserve organic, non-glacial sediments throughout the Holocene. In contrast, Loon and Iceboom lakes are “threshold lakes,” positioned to capture glacial meltwater at times during the late Holocene when the ice margin expanded beyond its present position. Loon Lake lies ~0.4 km from the Historical moraine (the Little Ice Age late Holocene maximum) and 3 km from the present-day ice sheet margin, and is free of ice-sheet meltwater today (Figs. 1 and 2). Iceboom Lake, which lies ~4 km from the present-day ice margin, was receiving meltwater from the ice sheet through much of the 20th century A.D. (as inferred from aerial photographs) but became non-glacial in the middle 1960s A.D. (Figs. 1 and 2) (Briner et al., 2010, 2011). Finally, Pluto Lake (Figs. 1 and 2) is situated immediately outboard of the early Holocene Marrait moraine. Pluto Lake initially deglaciated ~10.2 ka, received glacial meltwater during the brief ice sheet re-advance ~9.2 ka that deposited the Marrait moraine, and has been non-glacial since the ice sheet retreated from the moraine (Young et al., 2011a). Pluto Lake sedimentological data for the period following the Marrait retreat (i.e. since ~9.2 ka) are presented here.

Radiocarbon ages and basic physical stratigraphy from the threshold lakes have contributed to constraints on the local extent of the Greenland Ice Sheet through the Holocene, as described by Briner et al. (2010). Here, non-glacial sedimentary units recovered from those lakes are examined alongside comparable non-glacial records from North, Fishtote and Pluto lakes to assess regional coherence between lacustrine proxy records. We present sediment organic content and magnetic susceptibility measured downcore for all five lakes, and chironomid assemblage data from North and Fishtote lakes. For North Lake, where both geochronology and insect data were obtained at the highest resolution, biogenic silica abundances were also measured to complement those proxies. Geochronological and proxy data presented in this study are available online through the World Data Center for Paleoclimatology (http://www.ncdc.noaa.gov/paleo/data.html).

3. Methods

3.1. Coring

Cores were obtained during summer field seasons in 2008 and 2009, using a light percussion coring system (which is intended for sampling surface sediments and employs a check valve and no piston) deployed from a raft. Two cores intended for high-resolution analyses of recent sediments were sub-sectioned vertically in the field: Core 09-NOR-1 from North Lake was sectioned in 0.25-cm increments over the uppermost 10 cm and in 0.5-cm increments from 10 to 30 cm depth. Core 09-PLO-SC1 was sectioned in 0.25-cm increments from the surface to 17.5 cm depth. To preserve recent records intact, both cores were carefully recovered with undisturbed surface sediments overlain by clear lakewater. Remaining cores were decanted in the field and shipped whole, then split in the laboratory and kept in refrigerated storage.

3.2. Geochronology

All AMS ^{14}C ages were obtained on plant macrofossils picked from sediment samples, cleaned with de-ionized water and prepared at the INSTAAR (University of Colorado) Laboratory for AMS Radiocarbon Preparation and Research. Ages were calibrated using CALIB html version 6.0 and the INTCAL09 calibration curve (Stuiver et al., 2005). ^{210}Pb was measured in the surface cores from North and Pluto lakes by Alpha spectrometry at MyCore Scientific, Inc. (Ontario, Canada), and ^{210}Pb-based sediment ages were modeled by applying the constant rate of supply (CRS) model to the unsupported ^{210}Pb inventory (Appleby and Oldfield, 1978). Age-depth models were constructed by fitting the ^{14}C ages with spline functions using the CLAM code (Blaauw, 2010) in the statistical software package R. All age-depth models were run with 20,000 iterations; a cubic spline was used for Fishtote and Iceboom lakes, and a smooth spline was used for Loon, North and Pluto lakes.

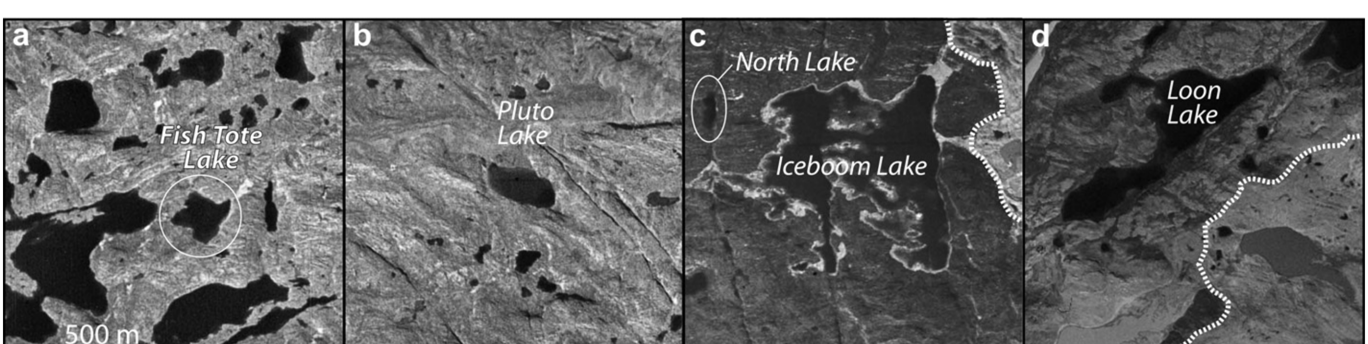

Fig. 2. Vertical air photographs of the five lakes: (a) Fishtote Lake, (b) Pluto Lake, (c) North and Iceboom lakes, and (d) Loon Lake. Up is north in all images, and scale bar applies to all images. Dashed white lines represent historical moraine. Image locations are shown in Fig. 1.

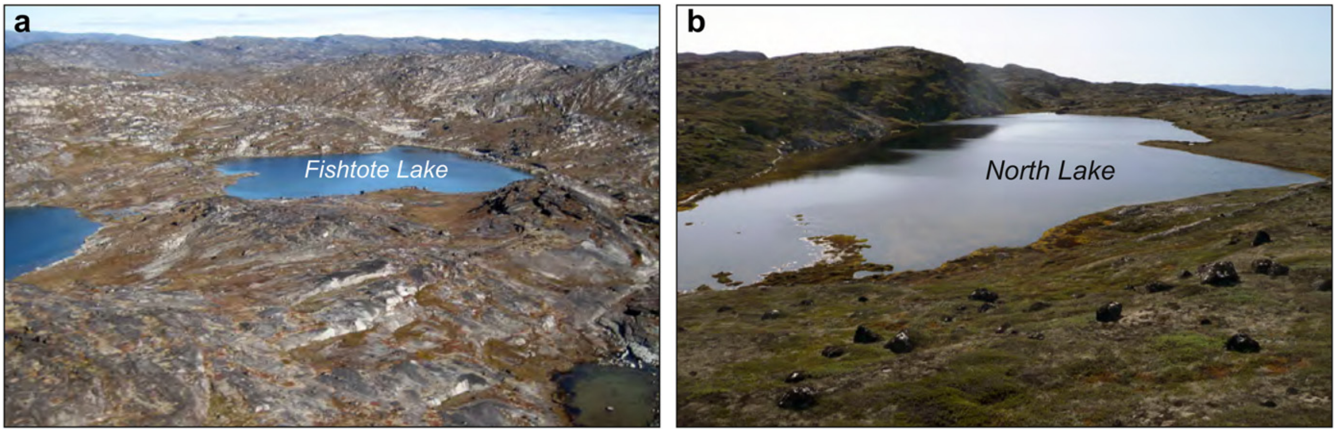

Fig. 3. Photographs showing the landscapes surrounding (a) Fishtote Lake and (b) North Lake.

Linear interpolation between the uppermost ^{14}C age and the modern surface was employed to estimate ages in the uppermost portions of the North, Loon, and Iceboom lake cores. Large apparent changes in sedimentation rates precluded employing this strategy for the Pluto or Fishtote lake cores. Proxy data from North Lake are derived from two cores – surface core 09-NOR-1, from which intact surface and recent sediments were subsampled in the field, and core 08-NOR-03, which extends to deglaciation of the site. Proxy data from the two North Lake cores are reported according to the two cores' independent chronologies (based upon ^{210}Pb for 09-NOR-1 and ^{14}C for 08-NOR-03).

3.3. Sediment composition

For all five lakes, the weight percent of sediment composed of organic material was estimated by loss-on-ignition (LOI). Subsamples of freeze-dried bulk sediment were ignited at 550 °C for two hours (Heiri et al., 2001). Freeze-dried bulk-sediment samples from North Lake were analyzed for biogenic silica ($bioSiO_2$) concentration following the methods described by Mortlock and Froelich (1989), slightly modified by using 10% Na_2CO_3 solution for $bioSiO_2$ extraction. A HACH DR/2000 spectrophotometer was used to measure $bioSiO_2$ concentration, which was then converted to weight percent SiO_2 of dry sediments. Weight percent mineral matter was estimated for North Lake as the residual of %LOI + % $bioSiO_2$. Magnetic susceptibility (MS), useful as a measure of the relative amount of minerogenic material in the sediment, was performed on all split cores at 0.5-cm intervals using a Bartington MS2E High Resolution Surface Scanning Sensor scanner connected to a Bartington MS2 Magnetic Susceptibility Meter.

3.4. Midge analyses and temperature reconstructions

Larval remains of chironomids, or "non-biting midges" (Diptera: Chironomidae), are abundant and well preserved in lake sediments at the study sites. A total of 41 sediment samples from North and Fishtote lakes were analyzed for chironomids. Chironomid analyses followed standard protocols (Walker, 2001). Wet sediment samples, ranging in volume from 0.5 to 2.0 cm^3, were deflocculated in warm 5% KOH for 20 min, then rinsed on a 100 μm mesh sieve. Chironomid head capsules were manually picked from a Bogorov sorting tray under a 40× power dissecting microscope, then mounted on slides using Euparal. All except one of the samples contained at least 50 whole identifiable head capsules (Heiri and Lotter, 2001); the uppermost sample from Fishtote Lake contained thirty-five.

July air temperatures were modeled using two independent methods: (1) a published weighted-averaging (WA) model developed for northeastern North America, based upon a geographically broad Eastern Canadian training set that includes sites from the Canadian Arctic islands west of Greenland (Walker et al., 1997; Francis et al., 2006), and (2) a published WA partial-least-squares (WA-PLS) model developed for Iceland, based upon a training set of more than 50 lakes in northwestern and western Iceland (Langdon et al., 2008). Both models use square-root transformed species data to model July air temperature, and all paleotemperatures were modeled using the software program C2 v 1.4.3 (Juggins, 2003).

Two versions of the Canadian WA model – one employing and one without tolerance downweighting – were used to model paleotemperature in order to test the sensitivity of the resulting temperature reconstructions to the common practice of tolerance downweighting. Previous work using these models in the Canadian Arctic has shown that temperature inferences derived from fossil samples with either very high or very low percentages of indicator taxa (taxa with narrow temperatures tolerances) can vary substantially depending upon whether tolerance downweighting is employed (Axford et al., 2011). Both versions of the Canadian model used inverse deshrinking. The Canadian model with tolerance downweighting (WAT model) has a cross-validated r^2 (r^2_{jack}) of 0.88 and a root mean squared error of prediction (RMSEP) of 1.5 °C; without tolerance downweighting, the WA model has r^2_{jack} of 0.87 and RMSEP of 1.6 °C. The Canadian transfer function has previously been used to reconstruct Holocene paleotemperatures at two lakes in West Greenland (Wooller et al., 2004, in southwest Greenland; and previously presented low-resolution results from North Lake in; Young et al., 2011b), and Holocene and Last Interglacial temperatures at several lakes in the Canadian Arctic (Francis et al., 2006; Axford et al., 2009a, 2011). The Icelandic transfer function, a two-component WA-PLS model employing classical deshrinking, has r^2_{jack} of 0.66 and RMSEP of 1.1 °C. This transfer function has been used to reconstruct Holocene temperature changes at several sites in Iceland (Axford et al., 2007; Caseldine et al., 2006; cf. Axford et al., 2009b), and recently was validated in northwestern Iceland by a study comparing late Holocene transfer function-based paleotemperature reconstructions from a high-altitude lake with instrumental temperature data and historical glacier extents (Langdon et al., 2011). The Canadian and Icelandic training sets cover July air temperature gradients of ∼5–19 °C and ∼6–11 °C, respectively. To help assess whether the Icelandic and Canadian training sets contain appropriate modern analogs for downcore (fossil) assemblages from our study sites, squared chord distances

(SCDs) were calculated between each fossil assemblage and its closest modern analog in each training set. SCDs were calculated on untransformed species data using C2.

Taxa were enumerated to the most precise taxonomic level possible using the taxonomic designations of Brooks et al. (2007), with additional reference to Oliver and Roussel (1983), Wiederholm (1983) and Rieradevall and Brooks (2001), and were subsequently lumped using two different strategies to harmonize with the two employed training sets. For example, for temperature modeling based upon the Canadian training set (Francis et al., 2006), all Tanytarsini (including separately enumerated *Tanytarsus lugens* type and *Micropsectra* spp.) were lumped within Tanytarsini undifferentiated, and all morphotypes of *Cricotopus* and *Orthocladius* were lumped together as *Cricotopus/Orthocladius* spp. In contrast, several distinct morphotypes of Tanytarsini and *Cricotopus/Orthocladius* were counted separately for temperature modeling based upon the Icelandic training set, which utilizes a higher level of taxonomic resolution (Langdon et al., 2008). All fossil taxa are represented in the training sets, with three exceptions: *Oliveridia/Hydrobaenus* is not included in the Iceland training set, so fossil *Oliveridia/Hydrobaenus* (present in two downcore samples from Fishtote Lake) were counted as *Pseudodiamesa* for temperature modeling using the Icelandic dataset, in accordance with the protocol used in past studies on Iceland (Axford et al., 2007; Langdon et al., 2011). To test the sensitivity of reconstructions to this strategy, we also modeled temperatures with *Oliveridia/Hydrobaenus* and *Pseudodiamesa* both excluded entirely from the training set and downcore data; this had a maximum effect of 0.3 °C on individual reconstructions. *Paracladopelma* and *Metriocnemus* are not represented in the Canadian training set, so were excluded from fossil counts for modeling using the Canadian training set. All three species were present only at low abundances (<2%) and in only a few samples. *Oliveridia/Hydrobaenus* and *Paracladopelma* occurred only in Fishtote Lake sediments, and *Metriocnemus* only in North Lake sediments.

Subfossil chironomid assemblages have previously been characterized and used as paleoenvironmental indicators at several sites in Greenland (e.g., Bennike et al., 2000; Brodersen and Anderson, 2002; Brodersen and Bennike, 2003; Wooller et al., 2004; Wagner et al., 2005; Klug et al., 2009; Schmidt et al., 2011), with the majority of these studies taking qualitative approaches to interpreting assemblages and assemblage changes. One detailed quantitative investigation examined chironomid assemblages in the surface sediments of a transect of lakes representing a wide range of summer climate and hydrochemistry in the Sisimiut–Kangerlussuaq region (~250 km south of our study sites), and evaluated the correlations between chironomid assemblages and several environmental variables including temperature (Brodersen and Anderson, 2002; Brodersen, 2007). The transect covered a broad range of climate conditions, from coastal to arid continental, and thus a very broad range of Arctic lake environments, from dilute to oligosaline, chemically concentrated, and meromictic lakes. Temperature was found to be a predictor of chironomid assemblages along the Sisimiut–Kangerlussuaq transect and in a paleo-record from the region (Anderson et al., 2008), but its influence was confounded by the correlation between temperature and trophic variables, which varied dramatically along the transect and were themselves strong predictors of chironomid assemblages.

Chironomids are sensitive to a wide range of environmental variables and it can be difficult to decouple the independent effects of correlated environmental variables on species assemblages, as demonstrated in the Sisimiut–Kangerlussuaq studies. Nonetheless, many studies have found summer temperature to be the dominant predictor of chironomid species distribution (Eggermont and Heiri, 2011; Brooks et al., 2012). Chironomids are therefore well established and widely used as a paleotemperature proxy, especially in cold regions (see reviews by Brooks, 2006; Walker and Cwynar, 2006), including for the Holocene (Brooks et al., 2012). Quantitative paleotemperature reconstructions based upon chironomid assemblages, like quantitative paleoenvironmental reconstructions in general, are subject to the assumptions that species–environment relationships and relationships between important covariant environmental variables have remained stable through time (Birks et al., 2010). Encouragingly for the present study, recent work has shown that quantitative chironomid-based Holocene paleotemperature reconstructions using the Icelandic and Canadian training sets employed here often compare well with inferences from independent proxy records as well as chironomid-based temperature reconstructions from adjacent sites (Caseldine et al., 2006; Axford et al., 2007, 2009a; Langdon et al., 2010; Langdon et al., 2011). Here, we employ the same training sets used for those studies in Iceland and the Canadian Arctic to investigate the Holocene temperature history of West Greenland.

4. Results

4.1. Geochronology and sedimentation histories

The basal ^{14}C ages (Table 2; Fig. 4) from this suite of lakes, which span from near the coast of Disko Bugt to the present ice margin, provide minimum-limiting ages for deglaciation of each site, and the quality of these ^{14}C ages is supported by agreement with previously published glacial chronology studies in the region. The extrapolated ~10 ka basal age of Fishtote Lake is in good agreement with ^{10}Be ages of nearby bedrock, which average 10.2 ± 0.2 ka (Corbett et al., 2011; Young et al., 2011b), and similar to minimum-limiting ^{14}C ages for deglaciation obtained from raised marine sediments (9.9 cal ka) (Weidick and Bennike, 2007). Basal ^{14}C ages from North and Iceboom lakes of 7.3 cal ka are similar to ^{10}Be-based deglaciation ages for the surrounding landscape (7.4 ± 0.2 ka) (Young et al., 2011b). The 9.2-cal ka ^{14}C age of the early Holocene minerogenic layer in the Pluto Lake core, which presumably corresponds to the deposition of the adjacent Marrait moraine, is consistent with independent evidence for the age of the Marrait moraine (Weidick and Bennike, 2007; Young et al., 2011a).

Age models indicate that average sedimentation rates at the three non-glacial lakes were very slow over the last thousand years or more (Table 2; Fig. 4). Lead isotope data from North Lake (Fig. 4) confirm the preservation of modern and recent sediments at this site. We infer that North Lake experienced constant sedimentation throughout the late Holocene, but at much slower rates on average since ~2.5 ka than during the early to middle Holocene. In contrast, ^{210}Pb data from Pluto Lake suggest either a lack of recent sedimentation or disturbance of uppermost sediments at this site, despite careful recovery and subsectioning in the field, following the same well-established methods as for North Lake (Fig. 4). The uppermost ^{14}C age in the Pluto Lake core – 2.3 ka at 4 cm depth (Table 2) – provides further evidence for very slow average late Holocene sedimentation rates here. A similar result at Fishtote Lake (where the uppermost ^{14}C age at 5 cm depth is 1.9 ka) suggests very slow average late Holocene sedimentation rates at that site as well. Together, these three lake records indicate very slow accumulation of organic sediments in lakes near Ilulissat after 1.9 ka or later, compared with faster accumulation throughout the early and middle Holocene. Loon Lake, a threshold lake, resembles the non-glacial lakes in terms of sedimentation rate history, displaying slowing sedimentation during the late Holocene. Minerogenic sediments in the uppermost few centimeters of the Loon Lake core attest to the receipt of ice sheet meltwater late in the Holocene, but due to a lack of age control in the upper part of this core, the timing of glaciofluvial sediment

Table 2
Radiocarbon ages from lake sediment cores.

Core	Depth (cm)	Lab Number	Material Dated	Fraction Modern	δ13C (‰PDB)	Radiocarbon Age (^{14}C yr BP)	Calibrated Age (cal yr BP ± 2σ)
Loon Lake							
08LOO-1	20	CURL-10094	Plant macrofossils	0.6180 ± 0.0009	−37.7	3865 ± 15	4320 ± 90
08LOO-1	32	CURL-10104	Plant macrofossils	0.5604 ± 0.0010	−32.1	4655 ± 15	5390 ± 70
08LOO-1	46	CURL-10088	Plant macrofossils	0.5265 ± 0.0009	−34.5	5155 ± 15	5920 ± 70
08LOO-1	61	CURL-10101	Plant macrofossils	0.5206 ± 0.0008	−29.5	5525 ± 15	6340 ± 50
North Lake							
08NOR-3	23	CURL-10089	Plant macrofossils	0.7265 ± 0.0010	−28.1	2565 ± 15	2680 ± 60
08NOR-3	40	CURL-12613	Plant macrofossils	0.6746 ± 0.0013	−24.0	3160 ± 20	3400 ± 40
08NOR-3	61	CURL-12600	Plant macrofossils	0.5928 ± 0.0009	−24.9	4200 ± 15	4740 ± 90
08NOR-3	74	CURL-10091	Plant macrofossils	0.5562 ± 0.0010	−28.6	4715 ± 20	5450 ± 130
08NOR-3	100	CURL-12603	Plant macrofossils	0.4631 ± 0.0008	−28.8	6185 ± 15	7090 ± 80
08NOR-3	103	CURL-10092	Plant macrofossils	0.4006 ± 0.0008	−12.7	7350 ± 20	8160 ± 120
Fishtote Lake							
09FTL-SC2	2	CURL-12593	Plant macrofossils	0.7864 ± 0.0012	−21.8	1930 ± 15	1860 ± 40
09FTL-SC2	36	CURL-12606	Plant macrofossils	0.6438 ± 0.0009	−28.0	3540 ± 15	3810 ± 80
09FTL-SC2	65	CURL-12601	Plant macrofossils	0.4995 ± 0.0008	−24.0	5575 ± 15	6360 ± 50
09FTL-SC2	96	CURL-12608	Plant macrofossils	0.367 ± 0.0009	−27.6	8050 ± 20	8910 ± 120
Iceboom Lake							
08ICE-5	23	CURL-10083	Plant macrofossils	0.9591 ± 0.0015	−23.5	335 ± 15	390 ± 80
08ICE-5	36	CURL-10439	Plant macrofossils	0.7952 ± 0.0019	−27.8	1840 ± 20	1770 ± 60
08ICE-5	57	CURL-10434	Plant macrofossils	0.6098 ± 0.0015	−30.7	3980 ± 20	4470 ± 50
08ICE-5	70	CURL-10441	Plant macrofossils	0.4534 ± 0.0013	−30.5	6360 ± 25	7300 ± 120
Pluto Lake							
09PLO-1	4	CURL-12609	Plant macrofossils	0.7539 ± 0.0010	−29.7	2270 ± 15	2260 ± 80
09PLO-1	25	CURL-12599	Plant macrofossils	0.6232 ± 0.0012	−28.7	3800 ± 20	4170 ± 70
09PLO-1	50	CURL-12604	Plant macrofossils	0.4050 ± 0.0011	−14.9	7260 ± 25	8090 ± 70
09PLO-1	76	CURL-12594	Plant macrofossils	0.3584 ± 0.0009	−13.3	8245 ± 20	9210 ± 80

deposition is poorly constrained. Iceboom Lake, the other threshold lake, experienced an abrupt increase in sedimentation rate after ~400 yrs ago at the onset of glaciofluvial input.

4.2. Sediment composition

Magnetic susceptibility at each site (Fig. 5) declines to near-zero values with the onset of organic sedimentation in the early Holocene, recording landscape stabilization and the onset of biological production in the lakes. Relatively inorganic sedimentation resumed, as reflected by increases in MS, during the late Holocene at Loon and Iceboom lakes. This inorganic sedimentation is inferred to record the ice sheet's advance into the lakes' watersheds and the associated influx of glaciofluvial sediment (Briner et al., 2010). MS remained near zero throughout the Holocene in the non-glacial lakes.

Maximum Holocene LOI values in four of the five lakes are between 30 and 40%; maximum LOI values at Loon Lake are ~20% (Fig. 5). The oldest lakes, Pluto and Fishtote, both register early Holocene periods of high LOI centered ~9 ka and lasting 200–400 yrs, followed by declines to their lowest postglacial values ~8.5–8.2 ka. Organic sedimentation in Iceboom, North and Loon lakes began ~7.8, 7.2 and 6.9 ka, respectively – following the local deglaciation of those basins and after the aforementioned LOI variations in Pluto and Fishtote lakes.

All five lakes record increasing and/or relatively high LOI values from ~7 ka to ~4.3 ka, followed by abrupt drops in LOI, with low LOI values at all lakes between 3.9 and 3.0 ka (Figs. 5 and 8). This contemporaneous mid-Holocene drop in LOI at all five lakes is one of the most conspicuous features of the sedimentological record. LOI recovered to near-maximum values in all lakes after the major but transient mid-Holocene decline, then dropped to very low values in Loon and Iceboom with the late Holocene onset of glaciofluvial input to the two threshold lakes as the ice sheet expanded. North Lake experienced organic sedimentation throughout the mid- to late-Holocene, registering relatively stable intermediate LOI values from 3.4 ka to present.

$BioSiO_2$ trends in North Lake sediments broadly parallel trends in LOI (Figs. 5 and 8): Both $bioSiO_2$ and LOI values generally rise through the early Holocene section, and a mid-Holocene drop in $bioSiO_2$ mimics the regional drop in LOI. The late Holocene section is characterized by relatively stable values of both proxies. By definition, mineral matter follows opposite trends, with declining abundance throughout the early Holocene and a major, transient mid-Holocene increase in abundance (Fig. 8). Maximum $bioSiO_2$ abundances (~25 weight percent) occur throughout the late Holocene (following recovery from the transient mid-Holocene drop), whereas maximum LOI values occur in the mid-Holocene between ~6.2 and 4.2 ka.

4.3. Chironomid assemblages and paleotemperature reconstructions

Twenty different chironomid taxa were enumerated in North and Fishtote lake sediments (Fig. 6a and b). The range of chironomid taxa preserved at both sites is similar, but with some notable exceptions including the occurrence of *Oliveridia/Hydrobaenus* and *Paracladopelma* exclusively in Fishtote Lake, the greater dominance of Tanytarsini in Fishtote Lake, and the much greater abundance of Chironomini (*Chironomus* spp. and *Dicrotendipes*) and Tanypodinae (especially *Procladius*) at North Lake. These assemblage differences may be related to lake depth (Brodersen and Anderson, 2002), with Fishtote Lake being somewhat larger and deeper than North Lake (Table 1) and/or may reflect colder summer temperatures and less productive conditions at Fishtote Lake, consistent with its higher elevation, proximity to the coast, and less vegetated watershed (Figs. 1 and 3).

At North Lake, the earliest assemblage at 7.1 ka was dominated by *Micropsectra* and other Tanytarsini, *Procladius* and other Tanypodinae, and *Psectrocladius sordidellus* type (Fig. 6a). *Dicrotendipes* joined the assemblage ~6.2 ka and *Chironomus* spp. increased in abundance, with a corresponding relative decline in *Micropsectra*, *P. sordidellus* type and *Procladius*. The next major shift in the

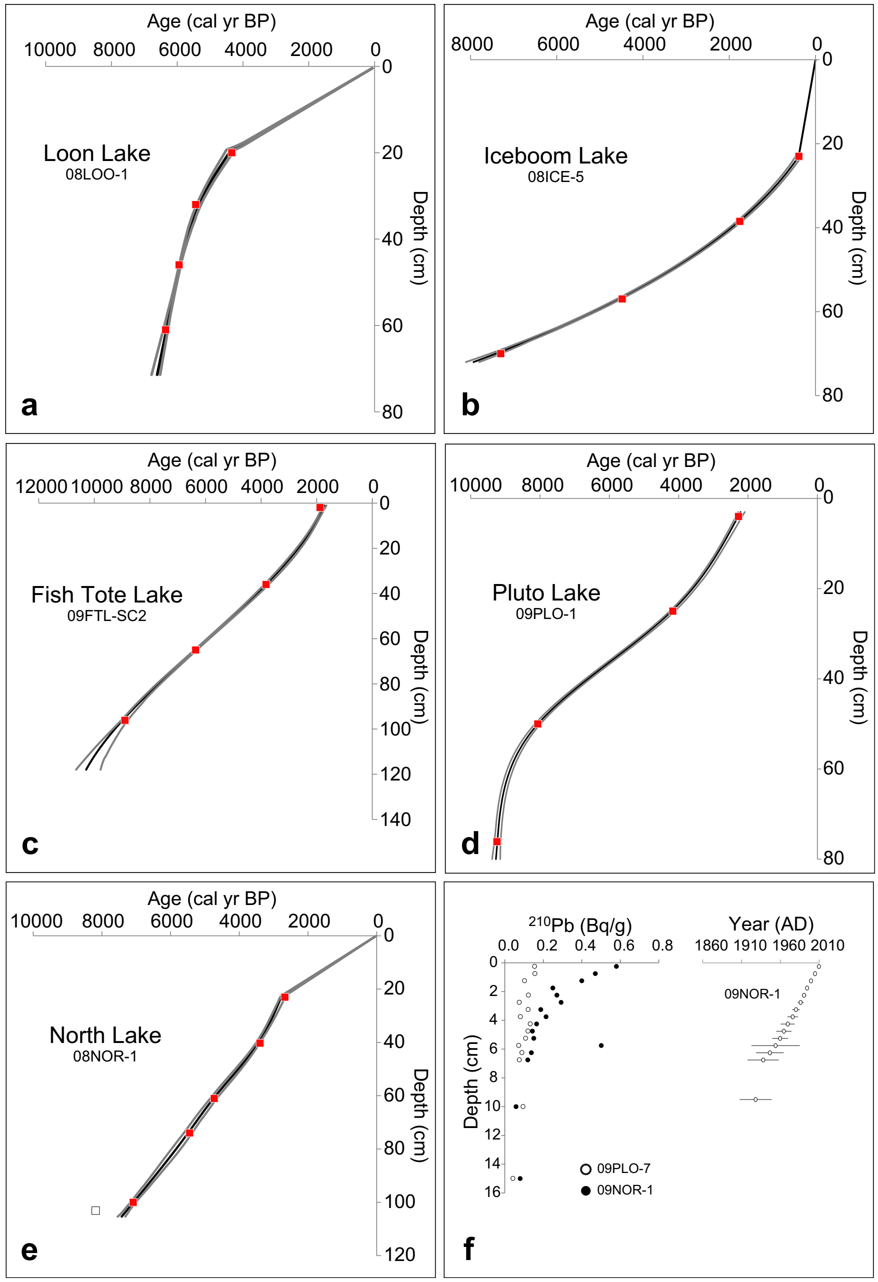

Fig. 4. (a–e) ^{14}C age models for the five study sites, with light gray lines depicting 95% confidence intervals for CLAM models. (f) ^{210}Pb measurements on surface cores from North and Pluto lakes, shown as filled and open circles, respectively; and resulting CRS age model for North Lake (standard deviations shown as horizontal bars).

assemblage occurred after ∼4.0 ka, when *Dicrotendipes* declined in abundance, *Heterotrissocladius* became important, and *Micropsectra* regained abundance. At ∼3.2 ka, *T. lugens* type appeared and the abundance of Tanypodinae, including *Procladius*, abruptly declined. *Dicrotendipes* disappeared from North Lake in the 19th century A.D. but re-appeared in the mid 20th century and has been present since then.

The Fishtote Lake record is dominated by Tanytarsini, which make up 69–94% of the assemblage in all Fishtote Lake samples (Fig. 6b). *Micropsectra* is especially dominant, composing as much as 78% of downcore assemblages. Early Holocene assemblages at Fishtote Lake were dominantly *Micropsectra*, *T. lugens* type, and *P. sordidellus* type. At ∼7.1 ka, *P. sordidellus* type tripled in abundance and *T. lugens* type declined. *Dicrotendipes* occurs in only one sample, ∼5.4 ka, midway through the period of dominance by *P. sordidellus* type. *P. sordidellus* type began to decline ∼4.6 ka, and the assemblage underwent a final shift ∼2.5 ka to greater abundance of *Heterotrissocladius* and *T. lugens* type, relatively low abundance of *P. sordidellus* type, and the appearance and persistence of *Oliveridia*/*Hydrobaenus*.

Dissimilarity calculations reveal that many, but not all, of the 41 samples from both cores have reasonable modern analogs in the existing training sets from Canada and Iceland. Ten of the 11 downcore samples from Fishtote Lake, and 21 of the 31 samples from North Lake, have SCDs <0.32 (the 10th percentile of the distribution of SCDs within the training set) from their closest analogs in the Canadian training set (Fig. 6a and b), indicating fair to good Canadian analogs for those samples. All samples from Fishtote Lake, and all but three of the samples from North Lake, have analogs closer than the 20th percentile within the Canadian training set

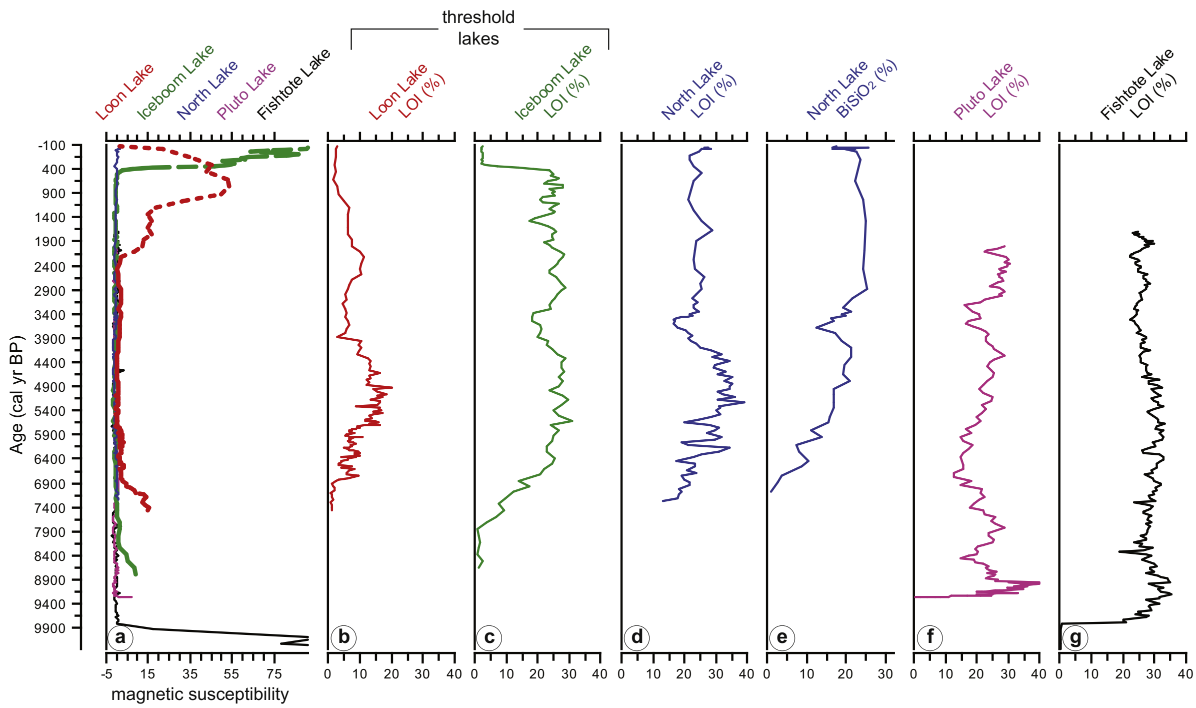

Fig. 5. Sediment composition data plotted vs. age for the five study lakes. (a) Magnetic susceptibility (MS, reported in cgs) data from all five lakes (Loon Lake shown as dotted line and Iceboom Lake as dashed line); (b, c, d, f, g) organic matter content estimated by weight percent loss-on-ignition (%LOI) for each lake; and (e) weight percent biogenic silica (% $bioSiO_2$) data from North Lake.

(i.e., <0.43). In both lakes, samples from the middle Holocene are the least similar to their closest analogs in the Canadian training set. Five samples from Fishtote Lake and 22 from North Lake have SCDs >0.39 (the 10th percentile within the training set) from their closest analogs in the Icelandic training set. The Icelandic training set covers a smaller climate gradient and narrower range of assemblages than the Canadian training set, and appears to offer less strong analogs to our downcore samples overall. In both lakes, samples with the poorest analogs in the Icelandic training set occur within the early and middle Holocene prior to 4 ka.

A comparison of the six different chironomid-based temperature reconstructions (from the two lakes, based upon the Langdon et al. (2008) Icelandic model and two versions of the Francis et al. (2006) Canadian model) reveals commonalities and differences between reconstructions (Fig. 7). Temperature anomalies (calculated as differences between downcore reconstructions and the reconstructed temperature based upon modern surface sediment assemblages) at North Lake are remarkably similar between the three models, with all models yielding reconstructions within model errors of each other and indicating the following major trends: (1) rising summer temperatures from the time of lake inception at 7.1 ka until 5.3 ka; (2) a period of peak warmth ~2–3 °C warmer than present between 5.9 and 4.0 ka; (3) a drop in temperatures between 4.0 and ~2.8 ka (with the rate of cooling varying between models, and possibly two phases of cooling ~4.0 and 3.0 ka); and (4) variable temperatures over the past millennium, with the coldest temperatures of the entire record (1.0–1.7 °C colder than present) occurring in the 19th century AD. The temperature difference between the 19th and 20th centuries reconstructed here is consistent with the instrumental temperature record from nearby Ilulissat (Vinther et al., 2006). Although reconstructed temperature anomalies are very similar between all three models, *absolute* temperatures inferred using the Icelandic transfer function are on average ~5 °C cooler than inferences based upon the Canadian transfer function throughout the Holocene. Absolute temperature inferences from the two WA models based upon the Canadian training set (one with and one without tolerance downweighting) are within model error of each other, although the model with tolerance downweighting yields lower temperature estimates for most of the Holocene and a smaller amplitude of overall Holocene temperature variation.

Temperature reconstructions from Fishtote Lake also indicate coldest temperatures in the late Holocene, including a conspicuous change in the chironomid assemblage and resulting inferred temperature drop at 3.0 ka. However, the WA (Canadian training set) results from this lake contrast with reconstructions from North Lake, in that relatively warm temperatures are inferred throughout the early to middle Holocene beginning with the oldest sample analyzed. The two Canadian WA models yield very similar results for the early to middle Holocene but diverge in the late Holocene, with tolerance downweighting yielding much colder temperatures in recent millennia after the cold stenotherm *Oliveridia/Hydrobaenus* appears (Fig. 6b). Unlike at North Lake, the Icelandic WA-PLS model suggests little overall trend in temperatures through the Holocene. Similar to North Lake, the Icelandic model yields absolute temperature estimates for Fishtote Lake that are consistently 4–5 °C lower than the estimates from the Canadian WA model (Fig. 7).

5. Discussion

5.1. The Holocene thermal maximum (HTM)

Chironomid-based temperature reconstructions from North Lake indicate a period of maximum Holocene warmth between ~6 and 4 ka, during which July air temperatures were likely 2–3 °C warmer than present. That North Lake chironomids provide a trustworthy reconstruction of temperature trends at

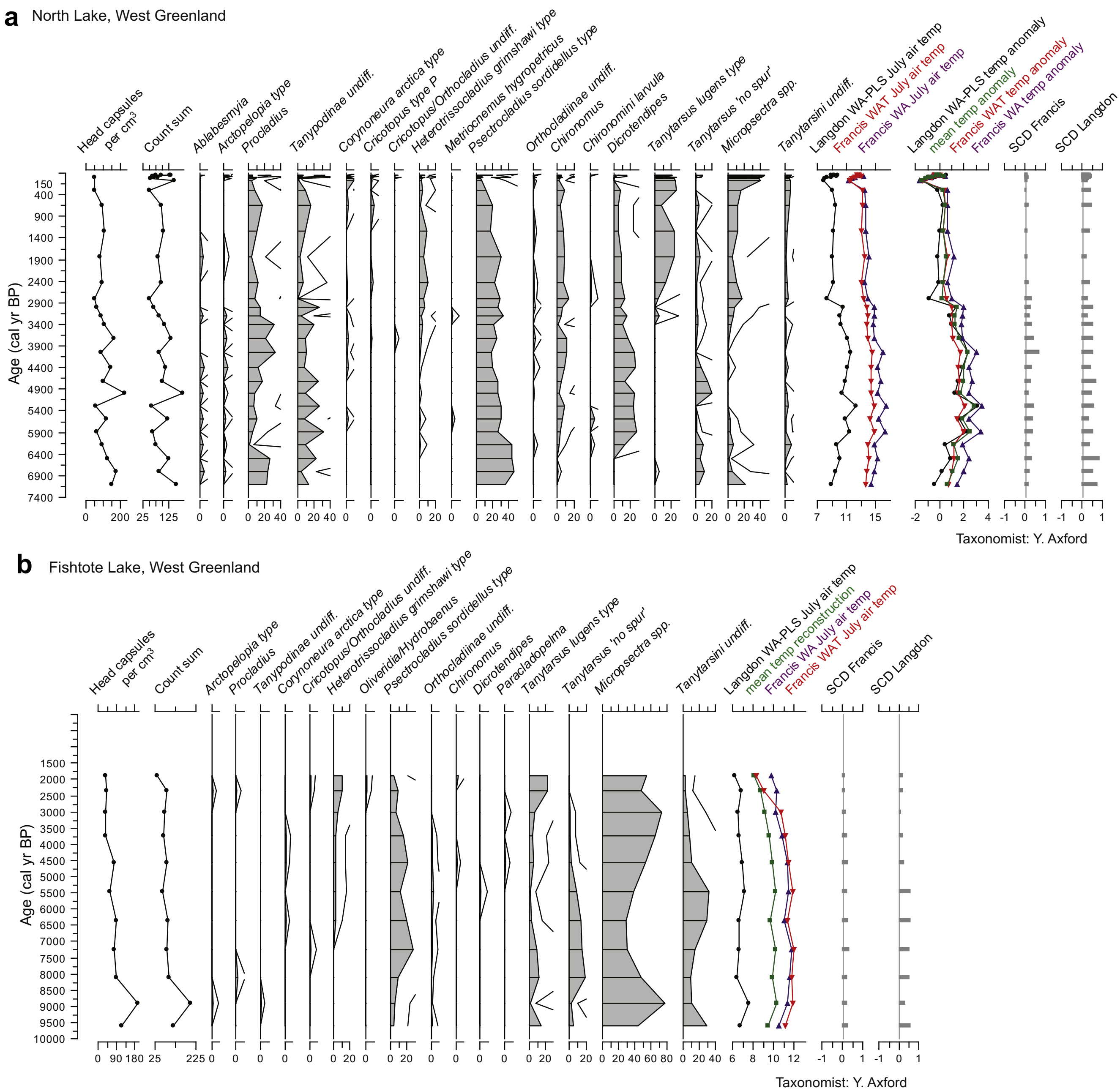

Fig. 6. Chironomid stratigraphic diagrams, showing head capsule concentrations (in whole head capsules per cm^3 wet sediment), number of identifiable whole head capsules enumerated per sample, percentage abundances of chironomid taxa (unfilled lines are 5× exaggeration), and temperature reconstructions based upon three different inference models for (a) North Lake and (b) Fishtote Lake. Both absolute July air temperature reconstructions and reconstructed July air temperature anomalies (vs. modern surface sample) are shown for North Lake. The Canadian model with tolerance downweighting ("Francis WAT" in the figure) has a RMSEP of 1.5 °C; the Canadian model without tolerance downweighting ("Francis WA") has a RMSEP of 1.6 °C; and the Icelandic WA-PLS model ("Langdon WA-PLS") has a RMSEP of 1.1 °C.

this site is supported by several lines of evidence: The same timing for maximum warmth and the same magnitude of warm anomaly are inferred regardless of which training set or statistical model is used, despite significant differences between these methods (e.g., major differences between training sets in the taxonomy of the abundant tribe Tanytarsini, and in the climate gradient covered by the two training sets). Qualitative assessment of chironomid assemblage shifts also suggests peak warmth ~6–4 ka, when assemblages were characterized by high abundance of the relatively thermophilous taxon *Dicrotendipes* and low abundances of types commonly associated with cold, oligotrophic conditions like *Heterotrissocladius* and *Micropsectra* (Fig. 6a). The reconstructed magnitude of warming between the 18th and 19th centuries is consistent with instrumental data from Ilulissat (Vinther et al., 2006). The presence of close modern analogs (as assessed by SCD) for many, but not all, downcore samples in both training sets indicates a reasonable but imperfect match between downcore chironomid assemblages and potential analogs in these training sets. Furthermore, the period of maximum warmth reconstructed from chironomids at North Lake coincides or overlaps with peaks in organic matter concentration (LOI) in all five study lakes (Fig. 5). Increasing organic concentrations in sediments of these five lakes could have resulted directly from rising lacustrine and terrestrial

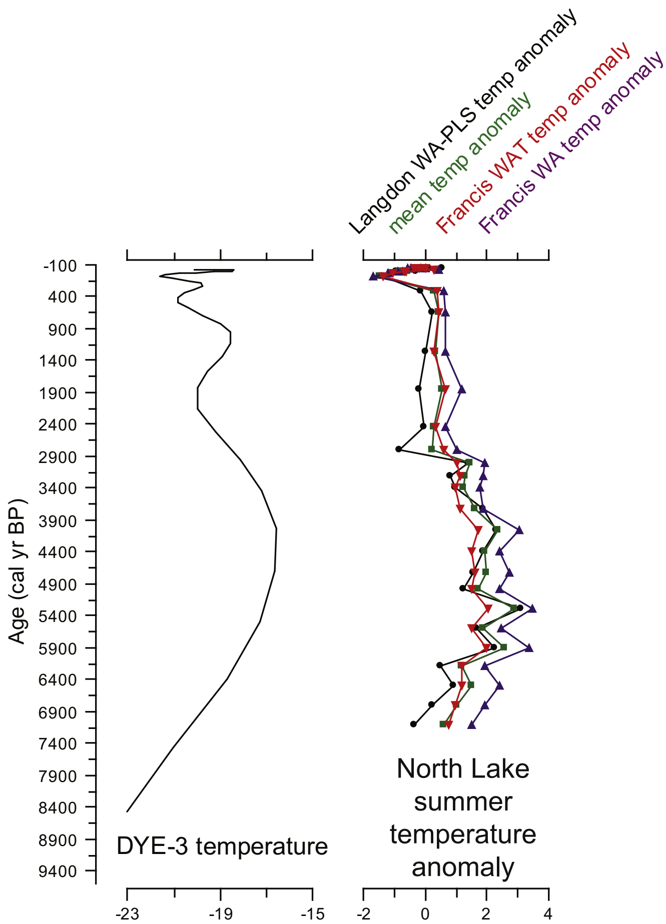

Fig. 7. Borehole-based paleotemperature record from DYE-3, Greenland (Dahl-Jensen et al., 1998), compared with reconstructed July air temperature anomalies from North Lake, inferred from chironomids using three different models as described in the text. Mean July air temperature anomalies are arithmetic means of the three model results.

productivity associated with warmer climate, and/or indirectly if warmer, more productive conditions reduced the oxygenation of lake waters and thus favored preservation of organic matter. This multi-site trend in organic deposition is unlikely to have resulted entirely from local ontogenetic trends independent of climate, given the range of ages of these lakes (9.7–6.5 ka; Table 1) and the preceding early Holocene rise and subsequent drop in LOI that occurred in the two oldest lakes.

Although temperature *anomaly* reconstructions for North Lake agree well between models, reconstructed *absolute* temperatures vary significantly between models, perhaps unsurprisingly given our experimental application of two very different non-local (Icelandic and Canadian) training sets to records from West Greenland. Absolute temperatures reconstructed in this study should therefore be interpreted cautiously, but estimates of temperature anomalies (i.e., differences relative to reconstructions from modern surface sediments) at North Lake appear robust. Temperature reconstructions from Fishtote Lake also vary significantly between models. All three reconstructions from Fishtote Lake suggest a slight peak in summer temperatures at 5.5 ka, and all are consistent with warmer temperatures in the early vs. late Holocene, but the reconstructions differ significantly in their estimates of temperature trends within the early to mid-Holocene (Fig. 6b). Chironomid assemblages at Fishtote Lake are very heavily dominated (up to 94%) by the taxonomically problematic and collectively eurythermic tribe Tanytarsini, which is split into several generic morphotypes in the Icelandic training set but lumped as a tribe in the Canadian dataset. As highlighted by Saulnier-Talbot and Pienitz (2010), Tanytarsini are abundant in many Canadian Arctic lakes, and interpretation of Tanytarsini-dominated assemblages there remains ambiguous. As the subfossil taxonomy and autoecological understanding of the Tanytarsini, including morphotypes of *Micropsectra* (which makes up as much as 74% of assemblages in Fishtote Lake), continues to improve (Brooks et al., 2007; Stur and Ekrem, 2011), Tanytarsini-dominated assemblages such as these at Fishtote Lake eventually may provide more confident paleoenvironmental interpretations. An additional challenge for interpreting chironomid assemblages at Fishtote Lake is the fact that, unlike for North Lake, temperature anomalies relative to estimates for present-day could not be calculated because we did not recover demonstrably modern surface sediments from Fishtote Lake, where sediment accumulation was very slow over the past ~2 ka.

To summarize results regarding the HTM from this study: Peak warmth is inferred from North Lake chironomids, and supported by high LOI values at all five study sites, to have occurred between 6 and 4 ka. Our multi-site results suggest that summer temperatures were warmer than present from the early Holocene through at least 3 ka, consistent with declining summer insolation through this period. The inferred timing of peak warmth is consistent with local ice sheet reconstructions, which indicate that the local ice sheet margin was at its most retracted Holocene position from 6 to 5 ka,

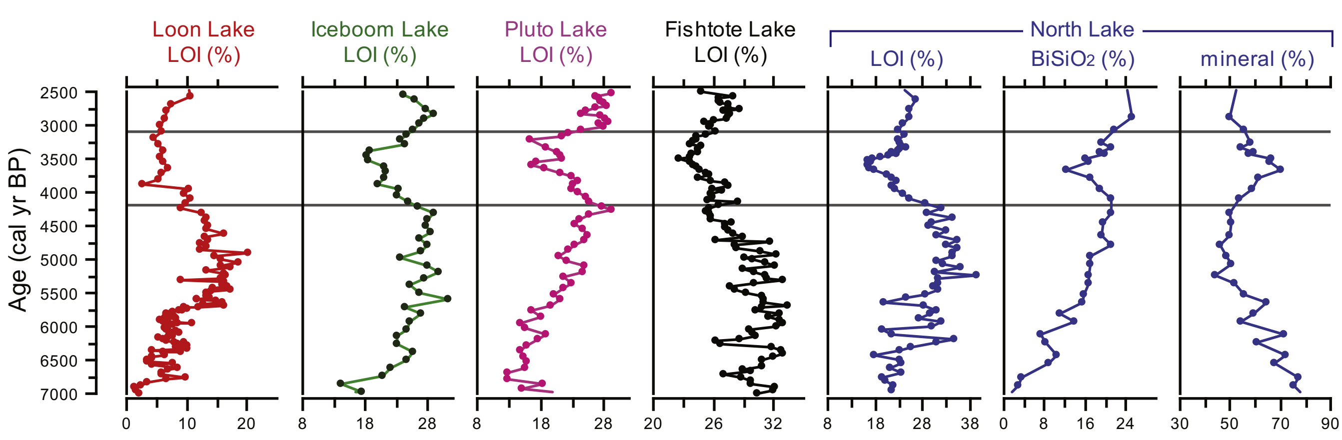

Fig. 8. Detailed view of loss-on-ignition (LOI) records from all study lakes, and biogenic silica ($bioSiO_2$) and mineral matter content records from North Lake, for the period over which all five lakes experienced organic, non-glacial sedimentation (~7–2.5 ka).

and that the ice sheet did not expand beyond its present-day margin until between ∼2.3 and 0.4 ka, depending upon exact location (Briner et al., 2010). That temperatures were warmer than present, and generally rising, in the early Holocene (as inferred from chironomids and from increasingly organic sedimentation at all sites) prior to the period of inferred maximum warmth agrees with glacial geologic evidence for rapidly retreating ice margins during that period, following a re-advance ∼8.2 ka (Young et al., 2011a, 2011b). Taken together, glacial geological and paleoecological data help constrain the sensitivity of the Greenland Ice Sheet to temperature change: The data indicate that the ice sheet margin in the Jakobshavn region underwent rapid retreat in the early Holocene following its 8.2 ka advance (Young et al., 2011a, 2011b), in a climate regime characterized by local summer temperatures no more than 2 °C warmer than present-day. Between 6 and 5 ka, when local summer temperatures were 2–3 °C warmer than present-day, the ice margin retracted an unknown distance behind its present position (Weidick et al., 1990; Weidick and Bennike, 2007; Briner et al., 2010; Young et al., 2011b).

Our data from the Jakobshavn region imply a somewhat later period of peak Holocene warmth than has been inferred from studies in the Kangerlussuaq region ∼250 km south. Around Kangerlussuaq, paleoecological data and other lacustrine proxies suggest peak warmth combined with reduced precipitation and attendant lake-level lowering between ∼7.2 and 5.6 ka (Anderson and Leng, 2004; Bennike et al., 2010). Water-balance modeling indicates that lake-level lowering during the warmest period around Kangerlussuaq was consistent with summer temperatures 2–3 °C warmer than present (the same magnitude of peak Holocene warmth inferred from chironomids at North Lake), combined with decreased mean annual precipitation (Aebly and Fritz, 2009). The inferred ∼1000-year difference in timing of peak warmth in the Jakobshavn versus Kangerlussuaq regions suggests local modulation of insolation forcing, e.g., different sensitivities of summer air temperatures at these sites to sea-surface conditions offshore, the variable climatic influence of local ice sheet margins, or perhaps later penetration of relatively warm, northbound West Greenland Current waters to the more northern Disko Bugt region.

The timing of maximum warmth inferred for all of these sites in West Greenland is delayed relative to peak summer insolation forcing, supporting the hypothesis that cold North Atlantic surface waters derived from rapidly receding Laurentide and Greenland ice sheets might have suppressed terrestrial temperatures in parts of the North Atlantic region during the earliest millennia of the Holocene (Kaufman et al., 2004; Kaplan and Wolfe, 2006; Carlson et al., 2008). Our data from the Jakobshavn region are consistent with the results of a recent modeling study, which estimated that the combined albedo and marine influences of the shrinking Laurentide Ice Sheet would delay maximum warmth along the west-central Greenland coast until 6–5 ka (Renssen et al., 2009). The timing of temperature changes inferred for North Lake also agrees remarkably well with borehole-based paleotemperature estimates from the Greenland Ice Sheet at DYE-3 (Dahl-Jensen et al., 1998) (Fig. 7), whereas the slightly earlier HTM inferred for the Kangerlussuaq region is in better agreement with borehole temperatures at GRIP (Dahl-Jensen et al., 1998).

Our results are in apparent disagreement with millennial-scale temperature trends inferred from Greenland ice core stable-isotope records, even when changes in ice sheet thickness are accounted for (Vinther et al., 2009). This apparent discrepancy between our paleoecological data and ice core isotopes – with the ice-core isotope records seemingly implying warmest temperatures in the earliest millennia of the Holocene (e.g., Vinther et al., 2009) – may record real spatial variability of temperature trends around Greenland, may reflect the different seasonal biases of different proxies and archives, and/or may support the notion that the effects of atmospheric reconfigurations on ice core isotopes partly overprints some Holocene temperature signals in isotopes of precipitation over the Greenland Ice Sheet (Fischer et al., 1998; Johnsen et al., 2001; Masson-Delmotte et al., 2005). Such results suggest that caution should be applied when extrapolating data from any single archive or proxy to represent general Holocene temperature trends around Greenland; trends undoubtedly varied both spatially and seasonally. As has been observed, this has important implications for ice-sheet model validation experiments, which rely upon accurate paleoclimate inputs to test the success of physical models in matching past ice-sheet configurations (e.g., Simpson et al., 2009; Applegate et al., 2012).

5.2. Late Holocene cooling and a ca 4.2-ka abrupt event

Collectively, results from our five study sites indicate declining temperatures through the late Holocene after ∼4 ka, a period characterized by cooling in many parts of the Arctic in response to declining summer insolation. Chironomid-based temperature reconstructions at North Lake place quantitative constraints on this cooling in West Greenland: All three models indicate a significant (0.5–1.5 °C) drop in summer temperatures ∼4.0 ka, when *Heterotrissocladius* rose in abundance at the expense of the relatively thermophilous taxon *Dicrotendipes*. This was followed by a second drop of similar magnitude at 3.0 ka, when Tanypodinae declined and Tanytarsini became more abundant (Figs. 6a and 7). Regional relative sea-level data indicate overall growth of this sector of the Greenland Ice Sheet after ∼3 ka (Long et al., 1999, 2006), and marine records from Disko Bugt record cooling after 3–2 ka (e.g., Perner et al., 2011), supporting the inference of cooling at this time.

Our inference models disagree about whether the drops in temperature ∼4 and 3 ka were gradual or abrupt. A strong but short-lived additional drop in temperatures is inferred by all models for the 18th and 19th centuries A.D., when chironomid assemblages at North Lake register the coldest temperatures of the entire record. This reflects the disappearance of *Dicrotendipes*, which re-appeared in 1950 A.D. and has been consistently present in North Lake sediments since then.

Downcore data from other lakes support these interpretations. At Fishtote Lake, the arrival of the cold stenotherm *Oliveridia*/*Hydrobaenus* and greater percentages of *Heterotrissocladius* and *T. lugens* type after 3 ka suggest a drop in summer temperatures (Fig. 6b). Very slow rates of organic sedimentation at the study sites during the last two millennia of the Holocene, indicated by age models for Fishtote, North and Pluto lakes, are consistent with low lake and landscape production and cool temperatures (Fig. 4). The two threshold lakes provide additional evidence for late Holocene cooling: The deposition of inorganic sediments in Loon Lake during the late Holocene indicates that the Greenland Ice Sheet margin advanced into the lake's watershed sometime after 4 ka (possibly ∼2.2 ka) (Briner et al., 2010, 2011). The ice sheet advanced into Iceboom Lake's watershed after ∼400 yrs ago and retreated to a position outside the lake's watershed between 1964 and 1985 A.D. (Briner et al., 2010), reinforcing the inference that recent centuries were the coldest since the deglaciation of Iceboom Lake ∼7.3 ka.

In addition to overall cooling since the HTM, two major transient climate events are recorded in late Holocene lake sediments from the study sites: The most recent – the Little Ice Age, which culminated at North Lake with 19th century summer temperatures that were colder than any other period in the record since deglaciation and ended when temperatures rose in the 20th century – is widely recognized as a cold event around the North Atlantic region and beyond, although it was heterogeneous in magnitude and timing. The earlier event is recorded by declines in the organic content (LOI) of sediments in all five study lakes between 4.3 and 3.2 ka, and a contemporaneous decline in algal production (bio-SiO_2) at the one site where bioSiO_2 was measured (Fig. 8). The fraction of lacustrine sediment made up of organic material is a complex function of many environmental variables, so LOI is generally unlikely to be a consistent recorder of any single environmental variable. However, the LOI records from all five of our study sites exhibit coherent major trends through the Holocene, suggesting a regional climatic driver behind these trends (Fig. 5).

Given the correlation between LOI and summer temperatures inferred for the study sites ~8.5–8.2 ka (during which an abrupt cold event occurred over central Greenland ~8.2 ka, and Jakobshavn Isbræ advanced) (Alley and Agustsdottir, 2005; Young et al., 2011a) and during mid-Holocene warming inferred from chironomids, it is tempting to interpret the period of low LOI and low bioSiO_2 from 4.3 to 3.2 ka as a cold event. However, whereas chironomids, LOI and bioSiO_2 data are all consistent with cooling at the beginning of this period, chironomid assemblages do not suggest warming/recovery at 3.2 ka when LOI and bioSiO_2 rebound. Rather than a transient decrease in organic and algal production, it is possible that lower LOI and bioSiO_2 concentrations during this interval could record a temporary increase in mineral matter deposition due to increased windiness, increased runoff, or a change in aeolian sedimentation that accompanied regional late Holocene ice sheet advance in response to declining temperatures.

The onset of this transient event in West Greenland overlaps with the timing of abrupt climate shifts documented at many sites far from West Greenland ~4.2 ka, including evidence for drought in central North America (Booth et al., 2005), glacier advance in western North America (Menounos et al., 2008), increased wetness and cooler conditions in northern Britain (Langdon et al., 2004; Langdon and Barber, 2005), and hydrologic changes implicated in cultural upheavals in the Middle East and south Asia (deMenocal, 2001; Staubwasser et al., 2003). More locally, Moros et al. (2006) record substantial environmental changes in Disko Bugt sediments at ~4 ka based on diatoms and sediment physical proxies. Masson-Delmotte et al. (2005) highlight an abrupt drop in GRIP deuterium excess at 4.5 ka, and suggest that this change in isotopes of precipitation over central Greenland may have recorded a shift in regional hydroclimate.

6. Conclusions

Based upon chironomid assemblages at North Lake, and supported by records of organic sedimentation in all five study lakes, we infer warmer-than-present temperatures by at least 7.1 ka and Holocene maximum warmth between 6 and 4 ka in central West Greenland near Jakobshavn Isbræ. Summer temperatures then declined by an estimated 2–3 °C through the late Holocene, and experienced an additional, short-term drop in the 18th and 19th centuries A.D. Temperature anomalies at North Lake were modeled using multiple training sets and multiple statistical methods, all of which yielded similar results, and records of organic content from all five study lakes support the chironomid-inferred timing of peak Holocene warmth. Although chironomid data from Fishtote Lake are generally consistent with these interpretations, chironomid-inferred temperatures from Fishtote Lake were deemed less reliable; assemblages at this site are heavily dominated by one tribe (Tanytarsini), which is known to be taxonomically problematic, and different statistical models and training sets yielded significantly different temperature reconstructions for this site.

The timing of inferred maximum warmth at North Lake and the other study sites coincides with minimum local Greenland Ice Sheet extent documented in previous studies, contributing to a coherent picture of millennial-scale regional summer temperature trends in the Jakobshavn region through the Holocene. Late Holocene and Little Ice Age cooling inferred here from midges and lake sediment composition are also in agreement with the regional glacial history. However, the timing and amplitude of maximum warmth inferred from lake-sediment data and ice sheet reconstructions around Jakobshavn contrasts with millennial-scale temperature trends inferred from isotopes in Greenland ice cores. This observation may reflect real spatial variability in Holocene climate, but could also support the hypothesis that millennial-scale Holocene temperature trends recorded by ice-core isotope records from central Greenland are partly overprinted by the isotopic effects of changing atmospheric circulation or changing seasonality of precipitation, in addition to changing ice sheet thickness. Either would argue for seeking temperature reconstructions from Greenland's ice-free margin and from a range of proxy methods when aiming to compare paleo-data between regions, validate general circulation models, or force ice sheet models.

We also report evidence for abrupt climate changes overprinted on these gradual insolation-driven climate changes during the Holocene: The two oldest study sites record declines in sedimentary organic content ~8.5 ka, which may be related to the 8.2 ka cooling over central Greenland and the recently documented advance of Jakobshavn Isbræ in response to that cooling. A regionally coherent transient climate change is recorded at all five study sites between 4.3 and 3.2 ka, which overlaps in timing with abrupt climate shifts documented at widespread sites from central North America to south Asia. Chironomid assemblages at both North and Fishtote lakes underwent significant shifts at 3 ka, involving multiple taxa. The coherence between lakes and taxa suggests that abrupt regional cooling ~3 ka drove those changes. The occurrence of abrupt climate shifts in West Greenland during the Holocene reinforces the notion that Holocene climate, which at high northern latitudes was primarily driven by gradual changes in summer insolation, exhibited non-linear sensitivities that may hold clues to the potential for abrupt future changes in climate.

Acknowledgments

Kristen Bartucci, Clayton Brengman, Otomo Darko, and Humza Shaikh contributed to laboratory analyses. Darrell Kaufman and Katherine Sides (Northern Arizona University) provided biogenic silica analyses. Chris Kuzawa, William Philipps, Heather Stewart, and Nicolás Young assisted with field work. We thank CH2M Hill Polar Services, including Robin Abbott, Mark "Sparky" Begnaud, and Ed Stockard, and the New York Air National Guard 109th Airlift Wing for help with field logistics. The Greenland Bureau of Minerals and Petroleum granted permission to collect samples. Chris Kuzawa and two anonymous reviewers provided helpful suggestions for improving this manuscript. This work was funded by the U.S. National Science Foundation (ARC-0909347 to Axford, ARC-0909334 to Briner, and BCS-0752848 to Briner and Axford) and the Initiative for Sustainability and Energy at Northwestern University (ISEN).

References

Aebly, F.A., Fritz, S.C., 2009. Palaeohydrology of Kangerlussuaq (Sondre Stromfjord), West Greenland during the last similar to 8000 years. Holocene 19, 91–104.

Alley, R., Agustsdottir, A., 2005. The 8k event: cause and consequences of a major Holocene abrupt climate change. Quat. Sci. Rev. 24, 1123–1149.

Alley, R.B., Fahnestock, M., Joughin, I., 2008. Understanding glacier flow in changing times. Science 322, 1061–1062.

Andersen, C., 2004. Nonuniform response of the major surface currents in the Nordic Seas to insolation forcing: implications for the Holocene climate variability. Paleoceanography 19, PA2003.

Anderson, N.J., Brodersen, K.P., Ryves, D.B., McGowan, S., Johansson, L.S., Jeppesen, E., Leng, M.J., 2008. Climate versus in-lake processes as controls on

the development of community structure in a low-arctic lake (South-West Greenland). Ecosystems 11, 307–324.
Anderson, N.J., Leng, M.J., 2004. Increased aridity during the early Holocene in West Greenland inferred from stable isotopes in laminated-lake sediments. Quat. Sci. Rev. 23, 841–849.
Anderson, N.J., Ryves, D.B., Grauert, M., McGowan, S., 2004. Holocene paleolimnology of Greenland and the North Atlantic islands (north of 60°N). In: Pienitz, R., Douglas, M.S.V., Smol, J.P. (Eds.), Long-term Environmental Change in Arctic and Antarctic Lakes. Springer, Dordrecht, The Netherlands, pp. 319–347.
Appleby, P.G., Oldfield, F., 1978. The calculation of 210Pb dates assuming a constant rate of supply of unsupported 210Pb to the sediment. Catena 5, 1–8.
Applegate, P.J., Kirchner, N., Stone, E.J., Keller, K., Greve, R., 2012. An assessment of key model parametric uncertainties in projections of Greenland Ice Sheet behavior. Cryosphere 6, 589–606.
Axford, Y., Briner, J.P., Francis, D.R., Miller, G.H., Walker, I.R., Wolfe, A.P., 2011. Chironomids record terrestrial temperature changes throughout Arctic interglacials of the past 200,000 yr. Geol. Soc. Am. Bull. 123, 1275–1287.
Axford, Y., Briner, J.P., Miller, G.H., Francis, D.R., 2009a. Paleoecological evidence for abrupt cold reversals during peak Holocene warmth on Baffin Island, Arctic Canada. Quatern. Res. 71, 142–149.
Axford, Y., Geirsdottir, A., Miller, G.H., Langdon, P.G., 2009b. Climate of the Little Ice Age and the past 2000 years in northeast Iceland inferred from chironomids and other lake sediment proxies. J. Paleolimnol. 41, 7–24.
Axford, Y., Miller, G.H., Geirsdóttir, Á., Langdon, P.G., 2007. Holocene temperature history of northern Iceland inferred from subfossil midges. Quat. Sci. Rev. 26, 3344–3358.
Bennike, O., 2004. Holocene sea-ice variations in Greenland: onshore evidence. Holocene 14, 607–613.
Bennike, O., Anderson, N.J., McGowan, S., 2010. Holocene palaeoecology of southwest Greenland inferred from macrofossils in sediments of an oligosaline lake. J. Paleolimnol 43, 787–798.
Bennike, O., Björck, S., Bocher, J., Walker, I.R., 2000. The Quaternary arthropod fauna of Greenland: a review with new data. Bull. Geol. Soc. Den. 47, 111–134.
Birks, H.J.B., Heiri, O., Seppe, H., Bjune, H.E., 2010. Strengths and weaknesses of quantitative climate reconstructions based on late-Quaternary biological proxies. Open Ecol. J. 3, 68–110.
Björck, S., Bennike, O., Rosen, P., Andresen, C.S., Bohncke, S., Kaas, E., Conley, D., 2002. Anomalously mild Younger Dryas summer conditions in southern Greenland. Geology 30, 427–430.
Blaauw, M., 2010. Methods and code for 'classical' age-modelling of radiocarbon sequences. Quat. Geochronol. 5, 512–518.
Booth, R.K., Jackson, S.T., Forman, S.L., Kutzbach, J.E., Bettis, E.A., Kreig, J., Wright, D.K., 2005. A severe centennial-scale drought in mid-continental North America 4200 years ago and apparent global linkages. Holocene 15, 321–328.
Briner, J.P., Stewart, H.A.M., Young, N.E., Philipps, W., Losee, S., 2010. Using proglacial-threshold lakes to constrain fluctuations of the Jakobshavn Isbrae ice margin, western Greenland, during the Holocene. Quat. Sci. Rev. 29, 3861–3874.
Briner, J.P., Young, N.E., Thomas, E.K., Stewart, H.A.M., Losee, S., Truex, S., 2011. Varve and radiocarbon dating support the rapid advance of Jakobshavn Isbrae during the Little Ice Age. Quat. Sci. Rev. 30, 2476–2486.
Brodersen, K.P., 2007. Chironomids (Diptera) from sub-saline lakes in West Greenland: diversity, assemblage structure and respiratory adaptation. In: Andersen, T. (Ed.), Contributions to the Systematics and Ecology of Aquatic Diptera—a Tribute to Ole A. Sæther, pp. 61–68.
Brodersen, K.P., Anderson, N.J., 2002. Distribution of chironomids (Diptera) in low arctic West Greenland lakes: trophic conditions, temperature and environmental reconstruction. Freshw. Biol. 47, 1137–1157.
Brodersen, K.P., Bennike, O., 2003. Interglacial Chironomidae (Diptera) from Thule, Northwest Greenland: matching modern analogues to fossil assemblages. Boreas 32, 560–565.
Brooks, S.J., 2006. Fossil midges (Diptera: Chironomidae) as palaeoclimatic indicators for the Eurasian region. Quat. Sci. Rev. 25, 1894–1910.
Brooks, S.J., Axford, Y., Heiri, O., Langdon, P.G., Larocque-Tobler, I., 2012. Chironomids can be reliable proxies for Holocene temperatures: a comment on Velle et al. (2010). Holocene. http://dx.doi.org/10.1177/0959683612449757.
Brooks, S.J., Langdon, P.G., Heiri, O., 2007. The Identification and Use of Palearctic Chironomidae Larvae in Palaeoecology: Quaternary Research Association Technical Guide 10. Quaternary Research Association.
Carlson, A.E., LeGrande, A.N., Oppo, D.W., Came, R.E., Schmidt, G.A., Anslow, F.S., Licciardi, J.M., Obbink, E.A., 2008. Rapid early Holocene deglaciation of the Laurentide ice sheet. Nat. Geosci. 1, 620–624.
Caseldine, C., Langdon, P., Holmes, N., 2006. Early Holocene climate variability and the timing and extent of the Holocene thermal maximum (HTM) in northern Iceland. Quat. Sci. Rev. 25, 2314–2331.
Corbett, L.B., Young, N.E., Bierman, P.R., Briner, J.P., Neumann, T.A., Rood, D.H., Graly, J.A., 2011. Paired bedrock and boulder 10Be concentrations resulting from early Holocene ice retreat near Jakobshavn Isfjord, western Greenland. Quat. Sci. Rev. 30, 1739–1749.
Dahl-Jensen, D., Mosegaard, K., Gundestrup, N., Clow, G.D., Johnsen, S.J., Hansen, A.W., Balling, N., 1998. Past temperatures directly from the Greenland Ice Sheet. Science 282, 268–271.
de Vernal, A., Hillaire-Marcel, C., 2006. Provincialism in trends and high frequency changes in the northwest North Atlantic during the Holocene. Glob. Planet. Change 54, 263–290.
deMenocal, P.B., 2001. Cultural responses to climate change during the Late Holocene. Science 292, 667–673.
Eggermont, H., Heiri, O., 2011. The chironomid-temperature relationship: expression in nature and palaeoenvironmental implications. Biol. Rev. Camb. Philos. Soc. 87, 430–456.
Fischer, H., Werner, M., Wagenbach, D., Schwager, M., Thorsteinnson, T., Wilhelms, F., Kipfstuhl, J., Sommer, S., 1998. Little ice age clearly recorded in northern Greenland ice cores. Geophys. Res. Lett. 25, 1749–1752.
Francis, D., Wolfe, A., Walker, I., Miller, G., 2006. Interglacial and Holocene temperature reconstructions based on midge remains in sediments of two lakes from Baffin Island, Nunavut, Arctic Canada. Palaeogeogr. Palaeoclimatol. Palaeoecol 236, 107–124.
Funder, S., Goosse, H., Jepsen, H., Kaas, E., Kjaer, K.H., Korsgaard, N.J., Larsen, N.K., Linderson, H., Lysa, A., Moller, P., Olsen, J., Willerslev, E., 2011. A 10,000-year record of Arctic Ocean sea-ice variability – view from the beach. Science 333, 747–750.
Heiri, O., Lotter, A.F., 2001. Effect of low count sums on quantitative environmental reconstructions: an example using subfossil chironomids. J. Paleolimnol 26, 343–350.
Heiri, O., Lotter, A.F., Lemcke, G., 2001. Loss on ignition as a method for estimating organic and carbonate content in sediments: reproducibility and compatibility of results. J. Paleolimnol 25, 101–110.
Hjort, C., Funder, S., 1974. The subfossil occurrence of *Mytilus edulis* in central East Greenland. Boreas 3, 23–33.
Jennings, A.E., Knudsen, K.L., Hald, M., Hansen, C.V., Andrews, J.T., 2002. A mid-Holocene shift in Arctic sea-ice variability on the East Greenland Shelf. Holocene 12, 49–58.
Johnsen, S.J., Dahl-Jensen, D., Gundestrup, N., Steffensen, J.P., Clausen, H.B., Miller, H., Masson-Delmotte, V., Sveinbjornsdottir, A.E., White, J., 2001. Oxygen isotope and palaeotemperature records from six Greenland ice-core stations: Camp Century, Dye-3, GRIP, GISP2, Renland and NorthGRIP. J. Quat. Sci. 16, 299–307.
Juggins, S., 2003. C2 User Guide: Software for Ecological and Palaeoecological Data Analysis and Visualization. University of Newcastle, Newcastle upon Tyne, UK.
Kaplan, M., 2002. Holocene environmental variability in southern Greenland inferred from lake sediments. Quat. Res. 58, 149–159.
Kaplan, M.R., Wolfe, A.P., 2006. Spatial and temporal variability of Holocene temperature in the North Atlantic region. Quat. Res. 65, 223–231.
Kaufman, D.K., Schneider, D.P., McKay, N.P., Ammann, C.M., Bradley, R.S., Briffa, K.R., Miller, G.H., Otto-Bliesner, B.L., Overpeck, J.T., Vinther, B.M., Arctic Lakes 2k Project Members, 2009. Recent warming reverses long-term arctic cooling. Science 325, 1236–1239.
Kaufman, D.S., Ager, T.A., Anderson, N.J., Anderson, P.M., Andrews, J.T., Bartlein, P.J., Brubaker, L.B., Coats, L.L., Cwynar, L.C., Duvall, M.L., Dyke, A.S., Edwards, M.E., Eisner, W.R., Gajewski, K., Geirsdottir, A., Hu, F.S., Jennings, A.E., Kaplan, M.R., Kerwin, M.N., Lozhkin, A.V., MacDonald, G.M., Miller, G.H., Mock, C.J., Oswald, W.W., Otto-Bliesner, B.L., Porinchu, D.F., Ruhland, K., Smol, J.P., Steig, E.J., Wolfe, B.B., 2004. Holocene thermal maximum in the western Arctic (0–180 degrees W). Quat. Sci. Rev. 23, 529–560.
Kelly, M.A., Lowell, T.V., 2009. Fluctuations of local glaciers in Greenland during latest Pleistocene and Holocene time. Quat. Sci. Rev. 28, 2088–2106.
Klug, M., Schmidt, S., Bennike, O., Heiri, O., Melles, M., Wagner, B., 2009. Lake sediments from Store Koldewey, Northeast Greenland, as archive of Late Pleistocene and Holocene climatic and environmental changes. Boreas 38, 59–71.
Langdon, P.G., Barber, K.E., 2005. The climate of Scotland over the last 5000 years inferred from multiproxy peatland records: inter-site correlations and regional variability. J. Quat. Sci. 20, 549–566.
Langdon, P.G., Barber, K.E., Lomas-Clarke, S.H., 2004. Reconstructing climate and environmental change in northern England through chironomid and pollen analyses: evidence from Talkin Tarn, Cumbria. J. Paleolimnol 32, 197–213.
Langdon, P.G., Caseldine, C.J., Croudace, I.W., Jarvis, S., Wastegard, S., Crowford, T.C., 2011. A chironomid-based reconstruction of summer temperatures in NW Iceland since AD 1650. Quat. Res. 75, 451–460.
Langdon, P.G., Holmes, N., Caseldine, C.J., 2008. Environmental controls on modern chironomid faunas from NW Iceland and implications for reconstructing climate change. J. Paleolimnol 40, 273–293.
Langdon, P.G., Leng, M.J., Holmes, N., Caseldine, C.J., 2010. Lacustrine evidence of early-Holocene environmental change in northern Iceland: a multiproxy palaeoecology and stable isotope study. Holocene 20, 205–214.
Long, A.J., 2009. Back to the future: Greenland's contribution to sea-level change. GSA Today 19, 4–10.
Long, A.J., Roberts, D.H., Dawson, S., 2006. Early Holocene history of the west Greenland Ice Sheet and the GH-8.2 event. Quat. Sci. Rev. 25, 904–922.
Long, A.J., Roberts, D.H., Wright, M.R., 1999. Isolation basin stratigraphy and Holocene relative sea-level change on Arveprinsen Ejland, Disko Bugt, West Greenland. J. Quat. Sci. 14, 323–345.
Masson-Delmotte, V., Landais, A., Stievenard, M., Cattani, O., Falourd, S., Jouzel, J., Johnsen, S.J., Jensen, D.D., Sveinsbjornsdottir, A., White, J.W.C., Popp, T., Fischer, H., 2005. Holocene climatic changes in Greenland: different deuterium excess signals at Greenland Ice Core Project (GRIP) and NorthGRIP. J. Geophys. Res-Atmos. 110
Mayewski, P., Rohling, E., Curtstager, J., Karlen, W., Maasch, K., Davidmeeker, L., Meyerson, E., Gasse, F., Vankreveld, S., Holmgren, K., 2004. Holocene climate variability. Quat. Res. 62, 243–255.

Menounos, B., Clague, J.J., Osborn, G., Luckman, B.H., Lakeman, T.R., Minkus, R., 2008. Western Canadian glaciers advance in concert with climate change circa 4.2 ka. Geophys. Res. Lett. 35
Moros, M., Jensen, K.G., Kuijpers, A., 2006. Mid- to late-Holocene hydrological and climatic variability in Disko Bugt, central West Greenland. Holocene 16, 357–367.
Mortlock, R.A., Froelich, P.N., 1989. A simple method for the rapid determination of biogenic opal in pelagic marine sediments. Deep-Sea Res. 36, 1415–1426.
Oliver, D.R., Roussel, M.E., 1983. The Insects and Arachnids of Canada: Part 11. The Genera of Larval Midges of Canada; Diptera: Chironomidae. In: Agriculture Canada Publication 1746. Ottawa.
Perner, K., Moros, M., Lloyd, J.M., Kuijpers, A., Telford, R.J., Harff, J., 2011. Centennial scale benthic foraminiferal record of late Holocene oceanographic variability in Disko Bugt, West Greenland. Quat. Sci. Rev. 30, 2815–2826.
Renssen, H., Seppa, H., Heiri, O., Roche, D.M., Goosse, H., Fichefet, T., 2009. The spatial and temporal complexity of the Holocene thermal maximum. Nat. Geosci. 2, 410–413.
Rieradevall, M., Brooks, S.J., 2001. An identification guide to subfossil Tanypodinae larvae (Insecta: Diptera: Chrionomidae) based on cephalic setation. J. Paleolimnol 25, 81–99.
Rignot, E., Velicogna, I., van den Broeke, M.R., Monaghan, A., Lenaerts, J., 2011. Acceleration of the contribution of the Greenland and Antarctic ice sheets to sea level rise. Geophys. Res. Lett. 38, L05503.
Robinson, A., Calov, R., Ganopolski, A., 2011. Greenland ice sheet model parameters constrained using simulations of the Eemian Interglacial. Clim. Past 7, 381–396.
Saulnier-Talbot, É., Pienitz, R., 2010. Postglacial chironomid assemblage succession in northernmost Ungava Peninsula, Canada. J. Quat. Sci. 25, 203–213.
Schmidt, S., Wagner, B., Heiri, O., Klug, M., Bennike, O., Melles, M., 2011. Chironomids as indicators of the Holocene climatic and environmental history of two lakes in Northeast Greenland. Boreas 40, 116–130.
Simpson, M.J.R., Milne, G.A., Huybrechts, P., Long, A.J., 2009. Calibrating a glaciological model of the Greenland ice sheet from the Last Glacial maximum to present-day using field observations of relative sea level and ice extent. Quat. Sci. Rev. 28, 1631–1657.
Staubwasser, M., Sirocko, F., Grootes, P.M., Segl, M., 2003. Climate change at the 4.2 ka BP termination of the Indus valley civilization and Holocene south Asian monsoon variability. Geophys. Res. Lett. 30
Stuiver, M., Reimer, P.J., Reimer, R.W., 2005. CALIB 5.0. WWW Program and Documentation. Available at: http://calib.qub.ac.uk/calib/.
Stur, E., Ekrem, T., 2011. Exploring unknown life stages of Arctic Tanytarsini (Diptera: Chironomidae) with DNA barcoding. Zootaxa, 27–39.
Sundqvist, H.S., Zhang, Q., Moberg, A., Holmgren, K., Kornich, H., Nilsson, J., Brattstrom, G., 2010. Climate change between the mid and late Holocene in northern high latitudes – part 1: survey of temperature and precipitation proxy data. Clim. Past 6, 591–608.
Vinther, B.M., Andersen, K.K., Jones, P.D., Briffa, K.R., Cappelen, J., 2006. Extending Greenland temperature records into the late eighteenth century. J. Geophys. Res-Atmos. 111
Vinther, B.M., Buchardt, S.L., Clausen, H.B., Dahl-Jensen, D., Johnsen, S.J., Fisher, D.A., Koerner, R.M., Raynaud, D., Lipenkov, V., Andersen, K.K., Blunier, T., Rasmussen, S.O., Steffensen, J.P., Svensson, A.M., 2009. Holocene thinning of the Greenland Ice Sheet. Nature 461, 385–388.
Wagner, B., Bennike, O., Bos, J.A.A., Cremer, H., Lotter, A.F., Melles, M., 2007. A multidisciplinary study of Holocene sediment records from Hjort Sø on Store Koldewey, Northeast Greenland. J. Paleolimnol 39, 381–398.
Wagner, B., Heiri, O., Hoyer, D., 2005. Chironomids as proxies for palaeoenvironmental changes in East Greenland: a Holocene record from Geographical Society Ø. Zeitschrift der Deutschen Gesellschaft für Geowissenschaften 156, 543–556.
Walker, I.R., 2001. Midges: Chironomidae and related Diptera. In: Smol, J.P., Birks, H.J.B., Last, W.M. (Eds.), Tracking Environmental Change Using Lake Sediments. Zoological Indicators, vol. 4. Kluwer, Dordrecht, The Netherlands, pp. 43–66.
Walker, I.R., Cwynar, L.C., 2006. Midges and palaeotemperature reconstruction – the North American experience. Quat. Sci. Rev. 25, 1911–1925.
Walker, I.R., Levesque, J., Cwynar, L.C., Lotter, A.F., 1997. An expanded surface-water paleotemperature inference model for use with fossil midges from eastern Canada. J. Paleolimnol 18, 165–178.
Weidick, A., Bennike, O., 2007. Quaternary glaciation history and glaciology of Jakobshavn Isbrae and the Disko Bugt region, West Greenland: a review. Geol. Surv. Den Greenl. 78
Weidick, A., Oerter, H., Reeh, N., Thomsen, H.H., Thorning, L., 1990. The recession of the inland ice margin during the Holocene climatic optimum in the Jakobshavn-Isfjord area of West Greenland. Glob. Planet. Change 82, 389–399.
Wiederholm, T., 1983. Chironomidae of the Holarctic region. Keys and diagnoses: part 1. Larvae. Entomologica Scand. Suppl. 19
Wooller, M.J., Francis, D., Fogel, M.L., Miller, G.H., Walker, I.R., Wolfe, A.P., 2004. Quantitative paleotemperature estimates from delta O-18 of chironomid head capsules preserved in arctic lake sediments. J. Paleolimnol. 31, 267–274.
Young, N.E., Briner, J.P., Axford, Y., Csatho, B., Babonis, G.S., Rood, D.H., Finkel, R.C., 2011a. Response of a marine-terminating Greenland outlet glacier to abrupt cooling 8200 and 9300 years ago. Geophys. Res. Lett. 38
Young, N.E., Briner, J.P., Stewart, H.A.M., Axford, Y., Csatho, B., Rood, D.H., Finkel, R.C., 2011b. Response of Jakobshavn Isbrae, Greenland, to Holocene climate change. Geology 39, 131–134.
Zhang, Q., Sundqvist, H.S., Moberg, A., Körnich, H., Nilsson, J., Holmgren, K., 2010. Climate change between the mid and late Holocene in northern high latitudes – part 2: model-data comparisons. Clim. Past 6, 609–626.